



Published in final edited form as:

Nat Med. 2013 July ; 19(7): . doi:10.1038/nm.3194.

Direct migration of follicular melanocyte stem cells to the epidermis after wounding or UVB irradiation is dependent on Mc1r signaling

Wei Chin Chou^{1,2}, Makoto Takeo^{1,2}, Piul Rabbani^{1,2}, Hai Hu^{1,2}, Wendy Lee^{1,2}, Young Rock Chung^{1,2}, John Carucci¹, Paul Overbeek³, and Mayumi Ito^{1,2}

¹The Ronald O. Perelman Department of Dermatology, New York University, School of Medicine, New York, New York, USA

²Department of Cell Biology. New York University, School of Medicine, New York, New York, USA

³Department of Cell Biology, Baylor College of Medicine, Houston, Texas, USA

Abstract

During wound healing, stem cells provide functional mature cells to meet acute demands for tissue regeneration¹. Simultaneously, the tissue must maintain stem cells to sustain its future regeneration capability. However, how these requirements are balanced in response to injury is unknown. Here we demonstrate that after wounding or ultraviolet type B irradiation, melanocyte stem cells (McSCs) in the hair follicle² exit the stem cell niche before their initial cell division. Upward migration of McSCs from the follicular niche occurs at the risk of stem cell depletion. McSCs migrate to the epidermis in a melanocortin 1 receptor (Mc1r)-dependent manner and differentiate into functional epidermal melanocytes, providing a pigmented protective barrier against ultraviolet irradiation over the damaged skin. These findings provide an example in which stem cell differentiation due to injury takes precedence over stem cell maintenance and show the potential for developing therapies for skin pigmentation disorders by manipulating McSCs.

Melanocytes produce pigment that is integral to both hair and skin color and that functions as a protective biological shield against harmful rays that cause DNA damage in skin cells³. Human skin contains melanocytes in the interfollicular epidermis, whereas epidermal melanocytes in mice skin disappear after birth and persist only in the hair follicle⁴. The bulge and secondary hair germ (sHG) of the hair follicle houses McSCs that are self-maintaining, slow cycling and competent at repopulating bulb melanocytes during the growing phase of the hair cycle^{2,5}. The idea that the skin may strategically reserve stem cells in a relatively protected niche that is far deeper than the skin surface was initially proposed in 1990⁶, and previous studies have provided evidence that epithelial stem cells in the hair follicle migrate to the epidermis and contribute to wound healing⁷⁻⁹. Notably, clinical

Correspondence should be addressed to: M.I. (mayumi.ito@nyumc.org).

Note: Supplementary information is available in the online version of the paper.

AUTHOR CONTRIBUTIONS

W.C. performed experiments, interpreted data and wrote the manuscript. M.T., P.R., H.H., Y.C. performed experiments and interpreted data. J.C. provided human skin and interpreted data. P.O. generated *Trp2-LacZ* mice and interpreted the data. M.I. performed experiments, interpreted data and wrote the manuscript.

COMPETING FINANCIAL INTERESTS

The authors declare no competing financial interests.

Reprints and permissions information is available online at <http://www.nature.com/reprints/index.html>.

observations in human skin suggest that hair follicles may provide epidermal melanocytes in the process of recovery from vitiligo^{10,11}, a hypopigmentation disease characterized by the loss of epidermal melanocytes. However, no experimental assays that model adult follicular melanocyte contribution currently exist. Consequently, no molecular mechanism has been identified that promotes this process. Elucidating ways to recruit melanocytes from the stem cell niche to the epidermis would have broad clinical utility for the treatment of pigmentary disorders such as vitiligo and piebaldism.

To determine whether McSCs in the hair follicle give rise to epidermal melanocytes, we monitored the movement of melanocytes after creating a 1-cm² excisional wound in the back skin of adult mice. We used *Trp2-LacZ* reporter mice in which melanocytes are tagged by LacZ expression¹². During the telogen phase, melanocytes were located exclusively in the bulge and sHG niche, which is composed primarily of epithelial cells^{2,13,14} (Fig. 1a). By 5 d after wounding, melanocytes began to migrate from the hair follicle niche through the upper follicular epithelium to the basal layer of the epidermis (Fig. 1a). We also observed the migration of melanocytes from the hair follicle to the epidermis by detecting Pax3, another marker that identifies McSCs and differentiated melanocytes¹⁵ (Fig. 1b). This migration occurred only in the wound periphery and not in hair follicles far from the wound site (Supplementary Fig. 1). We also labeled McSCs with GFP as label-retaining cells (LRCs) by taking advantage of their slow cycling nature² and using previously established mouse models^{8,16} (Fig. 1c). After wounding, LRCs migrated toward the epidermis (Fig. 1d). These results validate the notion that follicular McSCs move from the hair follicle to the epidermis after wounding.

The follicle-derived epidermal melanocytes were functional and had the ability to proliferate and express differentiation markers, including microphthalmia-associated transcription factor (MITF) and tyrosinase (Supplementary Fig. 2). Furthermore, ultraviolet type B (UVB) irradiation induced similar melanocyte migration, suggesting that McSCs residing in the hair follicle may contribute to ultraviolet light-induced skin tanning (Supplementary Fig. 3). We used UVB irradiation to induce similar melanocyte migration in mouse tail skin, where melanocytes are present in the epidermis. (Supplementary Fig. 3). We then used human scalp explant cultures to verify whether follicular melanocytes also migrate to the epidermis in human skin. We removed epidermal melanocytes by ablating the skin above the level of the sebaceous gland in the human scalp explants and then cultured the remaining denuded skin and analyzed whether follicular melanocytes can migrate to the re-epithelialized skin. By 8 d after culturing the explants, we found that melanocytes that were originally localized in the outer root sheath of the hair follicle migrated to the epidermis concomitant with re-epithelialization of the denuded skin (Supplementary Fig. 4). These observations are consistent with previous notions that human follicular melanocytes have the ability to populate the skin epidermis^{10,11}.

In some adult stem cell systems, such as hematopoietic stem cells, a discrete subset of stem cells that rarely divide under normal homeostatic conditions become activated only after injury to produce progeny¹⁷. We thus studied whether epidermal melanocytes originate from McSCs that normally give rise to hair melanocytes or whether they arise from a subset of specialized McSCs that are activated exclusively after injury. To address this question, we labeled McSCs that proliferated for hair bulb repopulation during the anagen phase by continuous BrdU injection in wild type mice right after induction of the anagen phase by hair depilation (Fig. 1e). We then created a wound on the back skin. By 6 d after wounding, BrdU⁺ McSCs were mobilized to the epidermis, demonstrating the dual capacity of a population of McSCs to give rise to both hair and epidermal melanocytes (Fig. 1f-i).

During examination of the wound peripheral region where upward melanocyte migration occurs, we noted that there was a rare population of approximately 50 unpigmented hair follicles surrounding the wound (present in 100% of wound samples examined) that is not present in non wounded mice (Fig. 2a–c). These unpigmented hairs did not regain pigment in subsequent hair cycles (Fig. 2d). Whole-mount analyses of these unpigmented hair follicles from *Trp2-LacZ* mice revealed a lack of melanocytes (Fig. 2b), showing that unpigmented hair production was due to the loss of McSCs. Analyses of whole-mount hair follicles at the wound periphery at an earlier time point during melanocyte migration identified hair follicles with a lower number of McSCs that was associated with the upward migration of melanocytes (Supplementary Fig. 5). This McSC loss in response to wounding is intriguing, as by definition adult tissue stem cells have the ability to self renew and maintain themselves while they give rise to differentiated progeny for tissue regeneration¹⁸. To address the mechanisms behind McSC loss, we first examined how McSCs are renewed while they produce progeny after injury. We continuously injected BrdU after wounding to label McSCs that proliferated to generate epidermal melanocytes. We found very few BrdU⁺ McSCs in the niche even at 4 d after wounding, when melanocytes began to appear in the epidermis (Fig. 2e and j). More than 80% of melanocytes migrating from the upper follicle (above the niche) to the epidermis were negative for BrdU, in contrast to the extensive labeling in the adjacent epithelial cells (Fig. 2f–h,j). These results demonstrate that McSCs exited the niche directly without undergoing proliferation. Moreover, we observed no cell death (apoptosis) of melanocytes in the niche during upward migration (data not shown). These results show that McSC depletion and the resultant hair graying in the wound periphery is due primarily to direct migration of McSCs from their niche. Similarly, shortly after UVB irradiation, we observed direct McSC migration (Supplementary Fig. 6) that was associated with a reduction in the number of McSCs (Supplementary Fig. 7). However, we never observed complete McSC depletion in the niche in the UVB-irradiated area, and we consistently did not find unpigmented hair formation after UVB treatment, suggesting that the remaining stem cells can replenish their niche and function in the following hair cycles.

To investigate the mechanisms underlying upward McSC migration, we focused on MC1R, which has a vital role in skin and hair pigmentation due to its essential role in the production of eumelanin^{19,20}. Furthermore, a recent report showed that Mc1r promotes melanoma cell migration *in vitro*²¹. Ligands of this pathway are stress hormones, including adrenocorticotrophic hormone (ACTH) and melanin-stimulating hormone (MSH), that are encoded by the *POMC* gene. It was previously reported that the amounts of these stress hormones are systemically and locally regulated by both mental and physical stress^{22,23}. Both human and mouse skin keratinocytes show an upregulation of *POMC* products, including ACTH and MSHs, after wounding or UVB irradiation^{24,25}.

To determine the role of Mc1r in McSC migration, we created a wound on Mc1r mutant mice that express nonfunctional Mc1r (*Mc1r^{e/e}* mice^{19,25}) and their littermate control mice (*Mc1r^{e/+}* and *Mc1r^{+/+}* mice). After injury, both *Mc1r^{e/e}* mice and control littermates re-epithelialized their wounds within a similar time period (control mice, 12.2 ± 0.9 d; mutant mice, 12.5 ± 1.2 d, mean ± s.d). Notably, *Mc1r^{e/e}* mice produced a lower number of epidermal melanocytes compared to control littermate mice (Fig. 3a–c). We also found that the number of McSCs that directly migrated to the epidermis without proliferation (BrdU incorporation) was lower in the mutant mice compared to in the control mice (Fig. 3d). Consistently, these mutant mice had less unpigmented hair, which was a result of McSC depletion in the wound periphery (Fig. 3e). Notably, *Mc1r^{e/e}* mice normally maintained McSCs (Supplementary Fig. 8) and repopulated hair melanocytes during the anagen phase in uninjured skin (Fig. 3f–h), showing that Mc1r is specifically required for the epidermal fate of McSCs.

Next, to examine whether a ligand for MC1R can promote the generation of epidermal melanocytes, we cultured skin explants harvested from *Trp2-LacZ* mice with the addition of ACTH. We irradiated skin explants with or without UVB (30 mJ cm⁻²) for 5 d in culture wells and assessed the number of epidermal melanocytes at 7 d after the start date of the culture (Fig. 3i). We found that although epidermal melanocytes were not produced in the absence of UVB irradiation even with the addition of ACTH (data not shown), ACTH markedly enhanced epidermal melanocyte production in the presence of UVB treatment compared to UVB-irradiated explants without the addition of ACTH. Conversely, ACTH had a significantly smaller effect on skin explants harvested from *Mc1r*^{e/e} mice as compared to explants from control littermates ($p < 0.05$). This suggests that ACTH may enhance melanocyte migration partly through Mc1r in this model. Notably, mouse melanocyte cultures with addition of ACTH had higher migration activity of melanocytes than cultures without addition of ACTH (Fig. 3j). Together these results suggest that ACTH can promote melanocyte migration and increase the number of epidermal melanocytes.

We then examined whether wound-induced epidermal melanocytes can revert back to follicular McSCs. We previously showed that after a large excision wound and subsequent re-epithelialization, *de novo* hair follicles develop in the center of the re-epithelialized wound in adult mice²⁶. To examine whether melanocytes that migrated to the wound epidermis could populate neogenic follicles, we first assessed the location of epidermal melanocytes in the wound area. Distribution of tyrosinase-related protein 2 (Trp2)⁺ cells revealed that most of the epidermal melanocytes are limited to the wound periphery and do not reach the center of the wound, where new follicles develop (Fig. 4a). This result agrees with the previous observation that most neogenic follicles lack pigment²⁶. Nevertheless, we found a few hair germs that developed in the outskirts of the cluster of *de novo* hair follicles that contained LacZ⁺ melanocytes (Fig. 4b–e). The reconstituted melanocytes in the bulge of neogenic hair follicles downregulated differentiation markers, including MITF, nuclear β -catenin and Mc1r, and had the ability to repopulate bulb melanocytes to sustain hair pigmentation in subsequent hair cycles, whereas unpigmented *de novo* hair follicles did not acquire pigment in the next hair cycle (Fig. 4f–h). This suggests that the melanocytes that repopulated the bulge are functionally equivalent to the original undifferentiated McSCs, and repopulation of the hair follicle niche by melanocytes probably occurs in concert with the development of hair follicles. In support of these findings, epidermal melanocytes derived from UVB-irradiated back skin from the *Trp2-LacZ* mice demonstrated the ability to become hair follicle bulge and bulb melanocytes in an *ex vivo* hair reconstitution assay (Fig. 4i,j) that includes processes analogous to hair follicle development^{27,28}. Our results show that follicle-derived epidermal melanocytes have the ability to become hair melanocytes.

Mechanisms for wound healing are finely tuned between those that promote stem cell differentiation to meet acute demands for tissue regeneration and those that promote stem cell maintenance. In the follicular McSC system, we found that the balance between the two mechanisms is tuned to promote the production of differentiated melanocytes. This bias may be reasonable, as pigmentation can help block the penetration of ultraviolet rays into the skin, which contributes to tumorigenesis^{29,30}. In adult mice, the hair coat shields the epidermis. It is possible that mice have evolved to acquire the ability to regenerate epidermal melanocytes to protect their skin in the event of injury or UVB irradiation.

Our results suggest that follicular McSCs may be an important source of epidermal melanocytes, which contribute to a wide range of skin pigmentation disorders when dysregulated, including postinflammatory hyperpigmentation, ultraviolet light-induced photodamage and melanoma. We demonstrated that McSCs in Mc1R mutant mice show profound defects in migration to the epidermis. This indicates that the Mc1R pathway, either intrinsically or extrinsically, has a vital role in the production of epidermal melanocytes

from McSCs. Modulation of the Mc1R pathway may be a new target in the development of effective treatments for skin pigmentation disorders (including vitiligo, postinflammatory hypopigmentation and postinflammatory hyperpigmentation) by influencing McSCs. Notably, Mc1R ligands (stress hormones) are known to promote skin pigmentation^{25,31}, yet paradoxically and anecdotally, they are believed to promote hair graying. We demonstrate that the same population of follicular McSCs can produce both hair and epidermal melanocytes and that the Mc1R pathway specifically promotes the epidermal fate of McSCs. Our results may provide insight into the relationship between stress hormones and hair graying and may serve as an initial step toward reconciling this paradox.

We expect that numerous other signals in addition to the ACTH-Mc1R pathway are involved in the regulation of McSC migration. Our characterization of McSC migration to the epidermis provides an important basis and opportunity to investigate the molecular mechanisms regulating the regeneration of epidermal melanocytes by follicular McSCs.

ONLINE METHODS

Mice

All animal protocols were approved by the Institutional Animal Care and Use Committee at NYU School of Medicine. *Mcl1^{cre}* mice (C57BL/6 background) and Wnt1-Cre; Rosa-stop–yellow fluorescent protein (YFP) mice were obtained from Jackson Laboratories, and *Trp2-LacZ* transgenic mice were generated in the laboratory of P.O.¹². For BrdU administration, mice were injected daily intraperitoneally with 10 mg ml⁻¹ BrdU at 50 µg per g body weight. Mice were maintained in the Smilow Central Animal Facility at NYU Langone Medical Center. Both male and female mice were used for all experiments.

Wounding experiments

For excisional wounds, the dorsal fur of 3-week-old mice was clipped. After mice were anesthetized with a ketamine-xylazine cocktail, a 1 cm² area of skin was excised. Mice were injected with the analgesic Buprenex. For epidermal ablation, after anesthesia, a 1-cm² area of skin was depilated using Nair and stripped with scotch tape 20 times.

UVB exposure

Dorsal fur of 7- to 8-week-old mice was clipped, and mice were anesthetized with a ketamine-xylazine cocktail. Mice were treated with 200 mJ cm⁻² UVB once daily for 5 consecutive days.

Detection of melanocyte LRCs

We adapted a method developed by Tumbar *et al.*⁸. Tyr-rtTA;tetO-H2B-GFP mice were maintained on 1mg/kg doxycycline-containing chow for 9 d starting at 1 d after birth. Label was chased by cessation of doxycycline treatment for 7 weeks.

X-gal staining and analyses

Wound epidermis or dorsal skin from *Trp2-LacZ* mice was harvested, and subcutaneous fat was removed using either scalpel blades or jewelers' forceps. Tissues were fixed in 4% paraformaldehyde for 30 min at 4 °C, and whole-mount X-gal staining was performed as described²⁶. We observed tissues every 30 min during X-gal incubation using a dissection microscope to terminate the X-gal reaction immediately after a clear signal was observed in the bulge and sHG area. The skin samples were analyzed either in whole-mount status using a dissection microscope or after sectioning the tissues and counterstaining with nuclear fast red. In whole-mount individual follicle analyses, X-gal–stained skin samples were incubated

serially in 20% glycerol, 1% KOH, 50% glycerol, 1% KOH and 100% glycerol overnight at room temperature. Hair follicles were then isolated under a dissection microscope (Axiovision Discovery V12) after X-gal staining. Z-stack images of individual hair follicles were taken with a Nikon Eclipse Ti inverted microscope at various depths. These images were processed to create a focused image and are shown as a three-dimensional surface image using the Extended Depth of Focus (EDF) function in the NIS-Elements software (Nikon).

Dihydroxyphenylalaline (DOPA) staining

Whole-mount epidermal sheets from wound areas were prepared as previously described²⁶. The epidermal sheets were incubated with DOPA for 6 h at 37 °C.

Tyramide staining

Staining was performed with modification of the procedure of Han *et al.*³³. Briefly, tissue samples were harvested in 70% ethanol. The tissues were then fixed in acetone and methanol (1:1) at -20 °C for 20 min. The tissues were incubated in 1× PBS for 5 min. Tissues were then incubated in a blocking solution of 3% hydrogen peroxide in 1× PBS at room temperature for 10 min and then in 5% goat serum in 1× PBS at room temperature for 20 min. Next, tissues were incubated in avidin solution followed by biotin solution at room temperature for 15 min each, with a wash in 0.1% Nonidet P-40 and PBS in between. Tissues were incubated in diluted biotinyl tyramide with amplification diluent (Perkin Elmer Life Science Products, Inc.) 1:50 at room temperature for 1 h and were then washed with 0.1% NP-40 and PBS. Tissues were incubated in horseradish peroxidase-conjugated streptavidin in 5% goat serum in 1× PBS (1:500) at room temperature for 1 h and then washed with 0.1% NP-40 and PBS. Tissues were then incubated in diaminobenzidine at room temperature for 10 min and then rinsed twice in distilled water. Tissues were stored in 50% glycerol at 4 °C.

Immunofluorescence

For paraffin sections, skin excised from mice was fixed overnight in 4% paraformaldehyde (USB Corporation, Cleveland, OH). After sequential dehydration in increasing concentrations of ethanol and xylene, the skin was embedded in paraffin. Paraffin sections were deparaffinized and microwaved in 10 mM Tris and 1 mM EDTA (pH 8.0) for antigen retrieval. For frozen sections, tissues were embedded in optimal cutting temperature (OCT) compound (Sakura, Torrance, CA) and stored at -80 °C. Sections were fixed in acetone and methanol for 10 min at -20 °C before immunostaining. For primary antibodies raised in mouse, sections were blocked for 1 h in blocking reagent (M.O.M. kit, Vector Laboratories). Tissue sections were then incubated with the primary antibodies listed below, followed by incubation with biotin-conjugated (1:100, Vector Laboratories, CA. cat#BA-2000, BA-9400, BA-9500 and BA-1000) or Alexa 488- or 594-conjugated secondary antibodies (Invitrogen, Carlsbad, CA. cat#A21202, A11005, A21206, A11055, A11058, A21208 and A21471). For the biotin-conjugated secondary antibodies, streptavidin conjugated to tetramethyl rhodamine isothiocyanate (TRITC) was used as the final amplification step. Sections were counterstained with DAPI (Vector Laboratories, Burlingame, CA). All immunofluorescence was observed and photographed on an upright AxioPlan, LSM 510, 710 (Zeiss, Germany). The primary antibodies used were: goat antibody to mouse Trp2 (1:100, Santa Cruz. Cat#sc-10451), antibody to mouse BrdU (1:100, BD Bioscience, cat#347580), rabbit antibody to K14 (Covance, cat#PRB-155P-100), mouse antibody to β -catenin (1:500, Sigma, cat#c7207), rabbit antibody to mouse Ki67 (1:100, Abcam, cat#ab15580), antibody to mouse Pax3 (1:50, DSHB, cat#Pax3-c), rabbit antibody to mouse tyrosinase (1:50, P. Manga), antibody to mouse MITF (1:20, Vector Laboratories. cat#VP-M650), rabbit

antibody to S100 (1:100, Dako, cat#Z0311) and antibody to Mc1R (1:50, Sigma, cat#M9193-50UL).

Mouse skin organ culture

Dorsal skin was collected from 21-day-old *Trp2-LacZ* mice, and connective tissue and subcutaneous fat were carefully removed using fine forceps and surgical blades. The skin was laid flat, dermis side down, on a nitrocellulose membrane with a 0.8- μm -diameter pore (Millipore). Four-millimeter skin punch biopsies were used for explants. Three explants were cultured per well of 24-well plates containing 500 μl of medium (DMEM, 10% FBS and 1 \times penicillin and streptomycin) at 37 $^{\circ}\text{C}$. Explants were irradiated with 30 mJ cm^{-2} UVB once a day for 5 d starting on the first day of culture using a hand-held lamp with a 6-W, 312-nm UVB bulb (Spectronics Corporation). On the seventh day of culture, explants were harvested and stained whole mount with X-gal as described above. ACTH was added beginning on the first day of culture to a concentration of 10 or 100 μM and was replenished every day. Five fields were counted per explant to calculate the average number of epidermal melanocytes under a dissection microscope (Zeiss, Discovery V12). The experiment was performed in triplicate.

Human scalp organ culture

We purchased deidentified human scalp skin from BIOPREDIC International (France). We also used deidentified human scalp skin that had been discarded anonymously after surgery. The procedure was approved by the Institutional Review Board of NYU as an exempt protocol. After cutting the scalp skin into 0.5 mm \times 0.5 mm pieces, the skin surface above the sebaceous gland, including the epithelium, was removed using a surgical blade (Miltex, Inc.) under a dissection microscope (Zeiss, Discovery V12). Individual denuded scalp explants were cultured in 24-well plates containing 500 μl of medium (DMEM, 10% FBS and 1 \times penicillin and streptomycin) for 8 d at 37 $^{\circ}\text{C}$. On the eighth day of culture, explants were harvested and processed for immunohistochemistry. The experiment was performed in triplicate.

Melanocyte migration assay

Melan-A cells³² (2.5×10^4) were suspended in mouse melanocyte starvation medium composed of DMEM with 0.5% FBS, 1% sodium pyruvate, 1% nonessential amino acids, 1 \times penicillin and streptomycin and 0.5% 12-*O*-tetradecanoylphorbol-13-acetate (TPA). The suspension was added to cell culture inserts (Falcon) containing a 8- μm polycarbonate filter. Cell culture inserts were transferred into 24-well plates containing complete mouse melanocyte medium composed of DMEM with 10% FBS, 1% sodium pyruvate, 1% nonessential amino acids, 1 \times penicillin and streptomycin and 0.5% TPA. ACTH (Phoenix pharmaceuticals) was added to a concentration of 1 or 10 μM to both the starvation and complete media. Cells were incubated at 37 $^{\circ}\text{C}$ in 5% CO_2 for 20 h. After removal of nonmigrating cells from the upper surface of the insert membrane by scrubbing, inserts were incubated in 10% formalin for 10 min at room temperature. Migrating cells were visualized by staining with 0.5% crystal violet for 30 min at room temperature and then counted under an inverted microscope (Nikon, TMS-F). Experiments were performed in triplicate.

Hair reconstitution assay

Eight-week-old *Trp2-LacZ* mice were irradiated with UVB (200 mJ cm^{-2}) for 5 d and euthanized at 3 d after the last day of UVB treatment. The fur was clipped, and the dorsal skin was harvested. After scraping the subcutaneous fat, the skin was cut into small pieces (0.5 cm^2) and incubated in 20 mM EDTA for 15 min at 37 $^{\circ}\text{C}$. The epidermis was separated using scalpel blades. This condition allows for the separation of the interfollicular epidermis

and infundibulum above the sebaceous glands. The epidermis was chopped finely in MEM for suspension cultures with 5% FBS and 100 mg l⁻¹ gentamycin sulfate. The epidermal mixture was stirred at room temperature for 20 min to detach basal cells. The obtained epidermal cell suspension was then filtered through 70- μ m pores. The cells were combined with the neonatal epidermal (1×10^6 cells) and dermal (1×10^7 cells) preparations prepared according to the procedure of Prouty *et al.*²⁸. The mixture of cells was centrifuged, and the pellet was resuspended in 30 μ l to be intradermally inoculated into nude mice.

Quantification and statistical analyses

For analysis of the number of bulb melanocytes, the percentage of BrdU+ melanocyte or the number and the percentage of unpigmented hair, at least 20 follicles, melanocytes or hair shafts were analyzed in tissues from at least three replicates. Data were analyzed using Student's *t* test.

Supplementary Material

Refer to Web version on PubMed Central for supplementary material.

Acknowledgments

Follicle-derived epidermal melanocytes were initially observed at G. Cotsarelis' laboratory at the University of Pennsylvania, and this work benefited greatly from the mentorship and generosity of G. Cotsarelis. We thank P. Manga at NYU for valuable discussion and providing Melan-a cells and antibody to mouse tyrosinase. We thank E. Hernando's lab at NYU for the protocol of the melanocyte migration assay. We thank the Microscopy Core of New York University (NYU) for use of confocal microscopes (NCRRS10 RR023704-01A1). M.T. is supported by the NYU Kimmel Stem Cell Center and NYSTEM training grant C026880. M.I. is supported by US National Institutes of Health National Institute of Arthritis and Musculoskeletal and Skin Diseases grant 1R01AR059768-01A1 and the Ellison Medical Foundation.

References

1. Fuchs E. Skin stem cells: rising to the surface. *J Cell Biol.* 2008; 180:273–284. [PubMed: 18209104]
2. Nishimura EK, et al. Dominant role of the niche in melanocyte stem-cell fate determination. *Nature.* 2002; 416:854–860. [PubMed: 11976685]
3. Lin JY, Fisher DE. Melanocyte biology and skin pigmentation. *Nature.* 2007; 445:843–850. [PubMed: 17314970]
4. Hirobe T. Histochemical survey of the distribution of the epidermal melanoblasts and melanocytes in the mouse during fetal and postnatal periods. *Anat Rec.* 1984; 208:589–594. [PubMed: 6731864]
5. Nishimura EK. Melanocyte stem cells: a melanocyte reservoir in hair follicles for hair and skin pigmentation. *Pigment Cell Melanoma Res.* 2011; 24:401–410. [PubMed: 21466661]
6. Cotsarelis G, Sun TT, Lavker RM. Label-retaining cells reside in the bulge area of pilosebaceous unit: implications for follicular stem cells, hair cycle, and skin carcinogenesis. *Cell.* 1990; 61:1329–1337. [PubMed: 2364430]
7. Taylor G, Lehrer MS, Jensen PJ, Sun TT, Lavker RM. Involvement of follicular stem cells in forming not only the follicle but also the epidermis. *Cell.* 2000; 102:451–461. [PubMed: 10966107]
8. Tumber T, et al. Defining the epithelial stem cell niche in skin. *Science.* 2004; 303:359–363. [PubMed: 14671312]
9. Ito M, et al. Stem cells in the hair follicle bulge contribute to wound repair but not to homeostasis of the epidermis. *Nat Med.* 2005; 11:1351–1354. [PubMed: 16288281]
10. Ortonne JP, MacDonald DM, Micoud A, Thivolet J. PUVA-induced repigmentation of vitiligo: a histochemical (split-DOPA) and ultrastructural study. *Br J Dermatol.* 1979; 101:1–12. [PubMed: 113025]

11. Cui J, Shen LY, Wang GC. Role of hair follicles in the repigmentation of vitiligo. *J Invest Dermatol.* 1991; 97:410–416. [PubMed: 1714927]
12. Zhao S, Overbeek PA. Tyrosinase-related protein 2 promoter targets transgene expression to ocular and neural crest-derived tissues. *Dev Biol.* 1999; 216:154–163. [PubMed: 10588869]
13. Tanimura S, et al. Hair follicle stem cells provide a functional niche for melanocyte stem cells. *Cell Stem Cell.* 2011; 8:177–187. [PubMed: 21295274]
14. Rabanni P, et al. Coordinated activation of Wnt in epithelial and melanocyte stem cells initiates pigmented hair regeneration. *Cell.* 2011; 145:941–955. [PubMed: 21663796]
15. Lang D, et al. Pax3 functions at a nodal point in melanocyte stem cell differentiation. *Nature.* 2005; 433:884–887. [PubMed: 15729346]
16. Chin L, et al. Essential role for oncogenic Ras in tumour maintenance. *Nature.* 1999; 400:468–472. [PubMed: 10440378]
17. Wilson A, et al. Hematopoietic stem cells reversibly switch from dormancy to self-renewal during homeostasis and repair. *Cell.* 2008; 135:1118–1129. [PubMed: 19062086]
18. Blanpain C, Fuchs E. Epidermal homeostasis: a balancing act of stem cells in the skin. *Nat Rev Mol Cell Biol.* 2009; 10:207–217. [PubMed: 19209183]
19. Robbins LS, et al. Pigmentation phenotypes of variant extension locus alleles result from point mutations that alter MSH receptor function. *Cell.* 1993; 72:827–834. [PubMed: 8458079]
20. Hunt G, Kyne S, Wakamatsu K, Ito S, Thody AJ. Nle4DPhe7 α -melanocyte-stimulating hormone increases the eumelanin:phaeomelanin ratio in cultured human melanocytes. *J Invest Dermatol.* 1995; 104:83–85. [PubMed: 7798647]
21. Seong I, et al. Sox10 controls migration of B16F10 melanoma cells through multiple regulatory target genes. *PLoS ONE.* 2012; 7:e31477. [PubMed: 22363655]
22. Ito N, et al. Human hair follicles display a functional equivalent of the hypothalamic-pituitary-adrenal axis and synthesize cortisol. *FASEB J.* 2005; 19:1332–1334. [PubMed: 15946990]
23. Slominski A, Wortsman J, Luger T, Paus R, Solomon S. Corticotropin releasing hormone and proopiomelanocortin involvement in the cutaneous response to stress. *Physiol Rev.* 2000; 80:979–1020. [PubMed: 10893429]
24. Vukelic S, et al. Cortisol synthesis in epidermis is induced by IL-1 and tissue injury. *J Biol Chem.* 2011; 286:10265–10275. [PubMed: 21239489]
25. D'Orazio JA, et al. Topical drug rescue strategy and skin protection based on the role of Mc1r in UV-induced tanning. *Nature.* 2006; 443:340–344. [PubMed: 16988713]
26. Ito M, et al. Wnt-dependent *de novo* hair follicle regeneration in adult mouse skin after wounding. *Nature.* 2007; 447:316–320. [PubMed: 17507982]
27. Lichti U, et al. *In vivo* regulation of murine hair growth: insights from grafting defined cell populations onto nude mice. *J Invest Dermatol.* 1993; 101 (Suppl):124S–129S. [PubMed: 8326145]
28. Prouty SM, Lawrence L, Stenn KS. Fibroblast-dependent induction of a murine skin lesion with similarity to human common blue nevus. *Am J Pathol.* 1996; 148:1871–1885. [PubMed: 8669473]
29. Pharoah PD. Shedding light on skin cancer. *Nat Genet.* 2008; 40:817–818. [PubMed: 18583973]
30. Gilchrist BA. Molecular aspects of tanning. *J Invest Dermatol.* 2011; 131:E14–E17. [PubMed: 22094400]
31. Inoue K, et al. Stress augmented ultraviolet-irradiation-induced pigmentation. *J Invest Dermatol.* 2003; 121:165–171. [PubMed: 12839577]
32. Bennett DC, Cooper PJ, Hart IR. A line of non-tumorigenic mouse melanocytes, syngeneic with the B16 melanoma and requiring a tumour promoter for growth. *Int J Cancer.* 1987; 39:414–418. [PubMed: 3102392]
33. Han R, Baden HP, Brissette JL, Weiner L. Redefining the skin's pigmentary system with a novel tyrosinase assay. *Pigment Cell Res.* 2002; 15:290–297. [PubMed: 12100495]

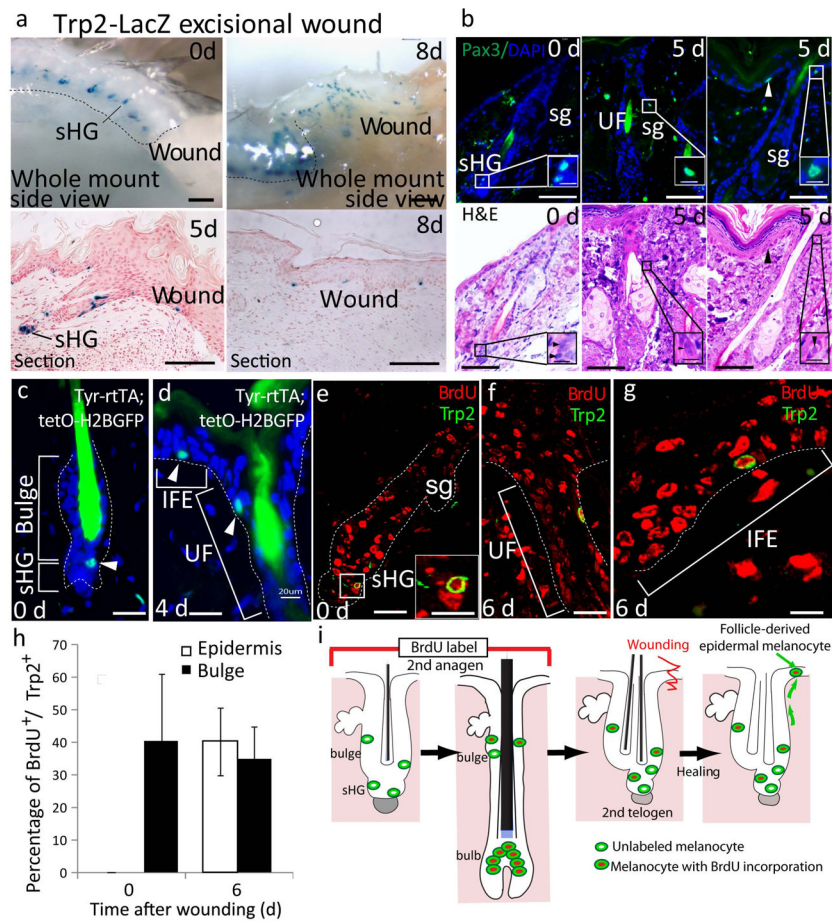


Figure 1. McSCs migrate from the hair follicle niche to the epidermis in response to injury or UVB irradiation. **(a)** X-gal-stained wound area of *Trp2-LacZ* mice before (0 d) and 5 or 8 d after wounding. **(b)** Pax3 (top) and H&E (bottom) staining of identical hair follicles at the indicated time points after wounding. UF, upper follicle; sg, sebaceous gland. Arrowhead indicates epidermal melanocyte. **(c,d)** Detection of melanocyte LRCs (arrowhead) in *Tyr-rtTA;TetO-H2B-GFP* mice^{8,16} at 0 d **(c)** and 4 d **(d)** after wounding. IFE, interfollicular epidermis. **(e-g)** BrdU- and Trp2-stained melanocytes before **(e)** and after **(f,g)** wounding and BrdU injection during the previous anagen phase. **(h)** Quantification of BrdU⁺Trp2⁺ melanocytes. The data is shown as the mean \pm s.d. **(i)** Experimental scheme of the BrdU labeling of the melanocytes shown in **e-g**. In **b** and **e**, the insets show the white boxed areas at higher magnification. In **a** and **c-g**, the dashed lines indicate the epidermis-dermis border. Scale bars, 500 μ m (**a**, top); 100 μ m (**a**, bottom); 25 μ m (**b**); 5 μ m (insets in **b**); 20 μ m (**c-g**); 10 μ m (inset in **e**).

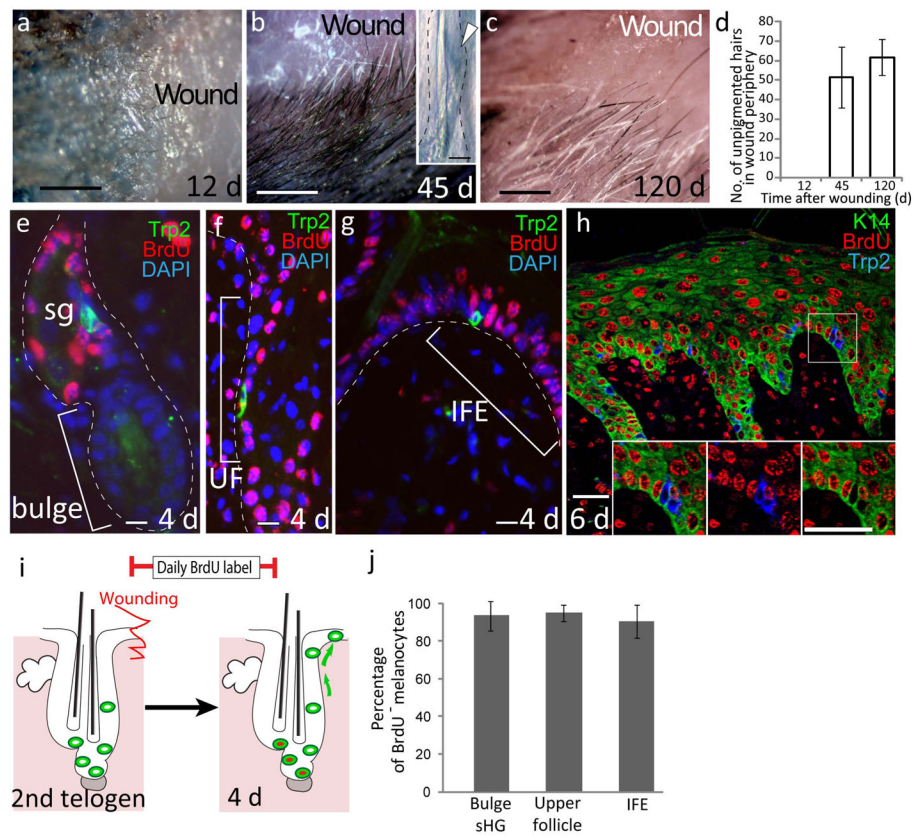


Figure 2. McSCs migrate directly from the hair follicle niche to the epidermis without proliferation. (a–c) Whole-mount images of the wound area and hair in the wound periphery of *Trp2-LacZ* mice at 12 d (a), 45 d (b) and 120 d (c) after wounding. The inset in b shows a bulge (arrowhead) in the unpigmented follicle stained with X-gal. (d) Quantification of the number of unpigmented hairs in the wound periphery. (e–g) Immunofluorescence for Trp2 and BrdU in skin from mice that were continuously injected with BrdU after wounding. (h) Immunofluorescence for K14, a marker for basal epidermal cells, Trp2 and BrdU. Insets show separate color images of the boxed area. (i) Schematic illustration of the results shown in e–h. (j) Quantification of BrdU⁺Trp2⁺ melanocytes in the wound periphery after 4 d. The dashed lines in b and e–g indicate the epidermis-dermis border. The data in d and j are shown as the mean ± s.d. Scale bars, 500 μm (a–c); 20 μm (eh and insets).

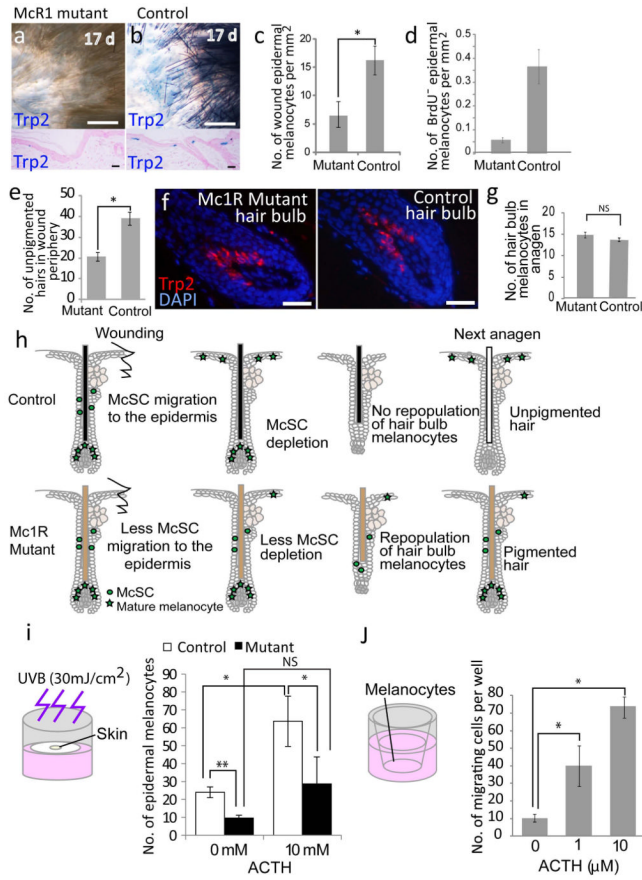


Figure 3. McSCs in *Mc1R* mutant mice show defects in migration to the epidermis. **(a,b)** X-gal-stained whole-mount and sectioned wound samples from *Mc1r^{el/e}; Trp2-LacZ* **(a)** and control *Trp2-LacZ* **(b)** mice after excisional wounding. **(c)** Number of *Trp2*⁺ epidermal melanocytes in the re-epithelialized area. **(d)** Quantification of BrdU⁻ epidermal melanocytes in the wound periphery after 5 d in *Mc1r^{el/e}* and wild-type control mice that were injected with BrdU after wounding. **(e)** Number of unpigmented hairs in the wound periphery after 30 d in *Mc1r^{el/e}* and wild-type control mice. **(f)** *Trp2* staining of hair follicle bulbs from depilated *Mc1r^{el/e}* and wild-type control mice at 6 d after anagen induction. **(g)** Quantification of *Trp2*⁺ bulb melanocytes. **(h)** Schematic representation of events after excisional wounding in *Mc1r^{el/e}* and control mice. **(i)** Number of epidermal melanocytes from UVB-treated explant assays with skin from *Trp2-LacZ* control mice and *Mc1r^{el/e}; Trp2-LacZ* mice cultured with or without ACTH. **(j)** *In vitro* melanocyte migration assay with melan-A cells³² treated with or without ACTH. The data in **c–e**, **g**, **i** and **j** are shown as the mean ± s.d. NS, not statistically significant. **P* < 0.05, ***P* < 0.01 determined by Student’s *t* test. Scale bars, 50 μm **(a,b, top)**; 20 μm **(a,b, bottom, f)**.

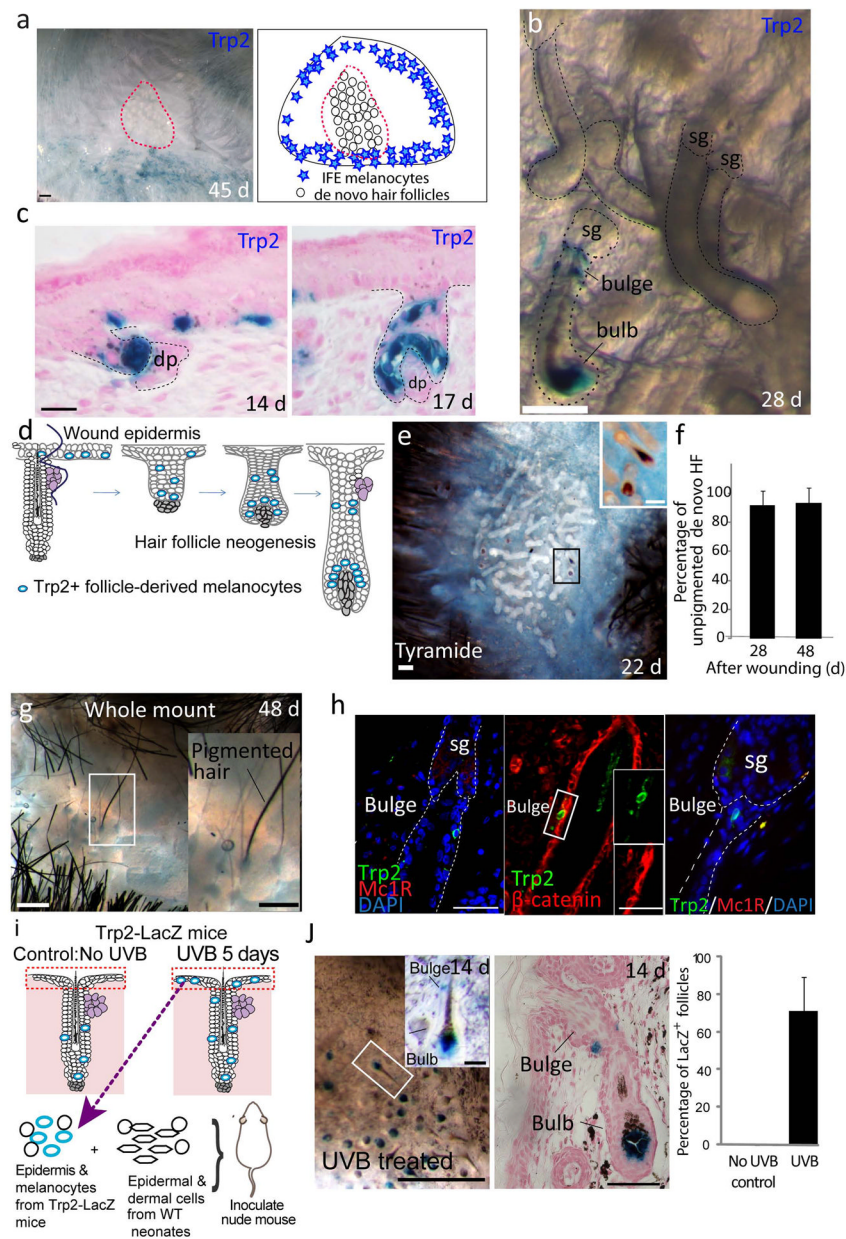


Figure 4. Epidermal melanocytes reconstitute McSCs in *de novo* hair follicles formed in the wound. **(a)** Epidermal view of the X-gal–stained wound area from wounded *Trp2-LacZ* mice (left) and an illustration of the location of epidermal melanocytes and the hair follicle neogenesis area (red dotted line) (right). **(b,c)** Views from the dermal side (**b**) and tissue sections (**c**) of neogenic follicles with *Trp2*⁺ melanocytes from wounded *Trp2-LacZ* mice. Dashed lines indicate outline of hair follicle. **(d)** Schematic illustration of melanocyte location during hair follicle neogenesis. **(e)** Whole-mount tyramide staining of wound epidermis at 22 d after excision showing pigment-producing melanocytes. **(f)** Quantification of unpigmented *de novo* hair follicles (HF) at 24 and 48 d after wounding. The data are shown as the mean \pm s.d. **(g)** Whole-mount image of a pigmented neogenic hair follicle at 48 d after wounding (the second anagen of neogenic hair follicles). **(h)** Staining of neogenic hair follicles sections with *Trp2* and the indicated melanocyte differentiation markers at 48 d after

wounding. **(i)** Scheme of the *ex vivo* hair reconstitution assay. **(j)** Whole-mount (left) and tissue section (center) of X-gal–stained reconstituted hair follicles from nude mice that were injected with an epidermal cell suspension from UVB-irradiated *Trp2-LacZ* mice. Right, quantification of LacZ⁺ hair follicles in nude mice injected with cells from UVB-treated or non–UVB treated *Trp2-LacZ* mice. The data are shown as the mean ± s.d. The insets in **e**, **g**, **h** and **j** show magnified views of the boxed areas. Scale bars, 500 μm (**a,e,g,j**, left); 25 μm (**b**); 20 μm (**c**); 50 μm (**h,j**, center).